Available online at www.sciencedirect.com
ScienceDirect
Journal of Power Sources 172 (2007) 229–234
JOURNAL OF POWER SOURCES
www.elsevier.com/locate/jpowsour

Short communication

Kinetics of oxygen reduction reaction on nanosized Pd electrocatalyst in acid media

J.J. Salvador-Pascual, S. Citalán-Cigarroa, O. Solorza-Feria *

Depto. Química, Centro de Investigación y de Estudios Avanzados del IPN, A. Postal 14-740, 07360 México, D.F., Mexico

Received 21 March 2007; received in revised form 21 May 2007; accepted 22 May 2007
Available online 31 May 2007

Abstract

Palladium electrocatalyst powder was prepared through $PdCl_2$ reduction with $NaBH_4$ in a THF solution at 0 °C. Characterization of the palladium phases, morphology and topography was performed by XRD, SEM, and AFM. Results from the X-ray diffraction (XRD) study showed evidence of nanocrystalline fcc hexagonal palladium formation with 4 nm in an average size. Electrocatalyst activity for the oxygen reduction reaction, ORR, was examined using cyclic voltammetry through rotating-disk electrode measurements in a 0.5 M H_2SO_4 electrolyte. Kinetic results suggest that the initial electron transfer is the rate-determining step. An apparent enthalpy of activation $\Delta H^{\circ\#} = 89.5 \pm 0.5\,\mathrm{kJ\,mol^{-1}}$ was calculated from electrochemical results at different temperatures. Based on current densities and the enthalpy of activation results, the nanosized Pd catalysts are significantly less active for the ORR than Pt and Ru electrocatalysts.

Keywords: Electrocatalysis; Palladium nanoparticles; Oxygen reduction; Rotating disk electrode; Enthalpy of activation

1. Introduction

The need of novel electrocatalytic materials is required in the large, energy intensive processes where the cost of generated electric power is a dominant factor. Electrocatalysts used for fuel cells have been extensively studied aiming the improvement of catalytic activity and greater stability at low cost. One of the major challenges in this field is the development of high-performance cathode catalysts in order to reduce the high overpotential present during the oxygen reduction reaction (ORR). Another aspect of interest, besides the activity and durability of the ORR electrocatalysts, is their selectivity for this reaction. Platinum and its alloys supported on carbon black are extensively used as cathode electrodes because they catalyze the four-electron reduction reaction of O_2 to form H_2O in low and medium temperature proton exchange membrane fuel cells, (PEMFC) [1–3]. These catalysts exhibit high specific features and stability when pure hydrogen is used as a fuel. However, Pt catalysts are scarce and expensive materials and therefore it is of great interest to find alternate Pt-free electrocatalysts for fuel cell applications. Non-platinum based material combinations supported on carbon black are also widely used as electrocatalysts for ORR on PEMFC [4–8]. Recently, several studies were aimed towards the study of interaction of oxygen with supported and unsupported Pd and Pt catalysts. These materials showed significant selectivity towards OH and/or O adsorption, thus decreasing the OH coverage on Pt and enhancing the ORR kinetics [9–17]. Metallic palladium presents considerable catalytic activity for the ORR in acid electrolyte [12] which preferentially proceeds through a four-electron pathway. It has been suggested that the metal–oxygen interaction may change as a function of the particle size at the nanoscale, thus enhancing the H_2O selectivity as been reported in several catalyzed reactions [18,19].

The aim of this work is to develop a methodology for the synthesis and characterization of palladium prepared nanoparticles through reduction of palladium chloride with $NaBH_4$ in THF media. The synthesized catalyst was characterized using X-ray diffractometer (XRD) and scanning electron microscopy (SEM). Cyclic voltammetry (CV) and rotating disk electrode (RDE) techniques were performed to evaluate the selectivity and to elucidate the mechanism of the catalytic activity on Pd-nanoparticles towards the oxygen reduction reaction in sulfuric acid electrolyte. The performance of the palladium catalyst was evaluated and compared to platinum in terms of catalytic

* Corresponding author. Tel.: +52 55 5061 3715; fax: +52 55 5061 3389.
E-mail address: osolorza@cinvestav.mx (O. Solorza-Feria).

0378-7753/$ – see front matter © 2007 Elsevier B.V. All rights reserved.
doi:10.1016/j.jpowsour.2007.05.093

activity. Additionally, the effect of temperature on the ORR kinetics for the Pd catalyst also was determined.

2. Experimental

2.1. Electrocatalyst preparation

Nanosized crystalline palladium was produced by a $NaBH_4$ reduction of $PdCl_2$ (0.86 mM) in a 100 mL Tetrahydrofuran (THF) (Aldrich) solution, as reported in literatures [20–22]. Briefly, the reaction system was charged with $PdCl_2$ and THF and the reducing agent ($NaBH_4$, 0.03 mM) slowly added drop-by-drop, while maintaining stirring at 0 °C under N_2 atmosphere for 16 h. After room temperature cooling, the reaction product was washed several times with distilled water to eliminate the produced sodium chloride. Afterwards, the powder was filtered, washed with ethylic ether and kept in a closed vessel in a desiccator at 293 K for 2 h. The product yield obtained was of 96%. The resulted dark-fine powder was used for optical and electrochemical measurements. Metallic and palladium powder (Aldrich) were acquired for electrochemical comparisons.

2.2. Physical characterization

The surface morphology of the particles was determined by scanning electron microscopy in a FEI Sirion XL30 analytical SEM operated at 20 kV. X-ray diffraction (XRD) was employed to determine the phases presented in the powder catalyst as synthesized. A D500 diffractometer (Siemens) with Co Kα radiation ($\lambda = 1.789007$ nm) was used for this purpose. A scanned range from 30° to 90°, with a stepwidth of 0.02° was used. Atomic force microscopy images were obtained in a JEOL scanning probe microscope mod. JSPM-4210 in tapping mode, with a resonant frequency of 150 kHz and Ultra-Sharp silicon cantilever NSC 12 was used to analyze the topography of the palladium sample.

2.3. Electrochemical characterization

The oxygen reduction reaction performance was evaluated in a 0.5 mol L^{-1} of sulfuric acid at temperature range between 30 and 80 °C in a thermostated controlled double-compartment cell. The working electrode and a Pt mesh counter-electrode were maintained in the same compartment. The reference electrode $Hg/Hg_2SO_4/0.5$ M H_2SO_4 (MSE = 0.65 V/NHE) was placed outside the cell, kept at room temperature and connected to a porcelain Lugging capillary. Potentials are referred to NHE. An EG&G Princeton Applied Research (PARC mod 273A) potentiostat was used for the electrochemical experiments. Cyclic voltammetry and Rotating disk electrode (RDE) measurements were conducted on a thin film catalysts deposited on a glassy-carbon disk electrode (0.38 cm^2) mounted in an interchangeable RDE holder (Pine Instruments). The glassy carbon working electrode disk was prepared according to a method reported previously [23,24]. A thin film was deposited from a solution prepared by adding 10 μL of a resulting suspension from a mixture of 75 μL of an alcoholic solution containing 5 μL of Nafion® (5 wt.%, Du Pont, 1000 EW) and 0.8 mg of Pd (10 wt.%/C). The estimated amount of catalyst on the glassy carbon electrode surface was about 1 mg cm^{-2}. The hydrodynamic experiments were recorded in the rotation rate range of 100–1600 rpm at 5 mV s^{-1}. During the ORR measurements an oxygen flux was maintained above the electrolyte surface.

3. Results and discussion

3.1. Physical characterization results

The X-ray diffraction of the palladium electrocatalyst is shown in Fig. 1. The powder electrocatalyst showed five diffraction peaks at about $2\theta = 40°$, 47°, 67°, 83° and 87° identified as single hexagonal fcc phase of palladium. The experimental pattern matches well with the standard crystallographic tables JCPDS card 00-046-1043. The broad feature in the low angle of the scattering region, suggests the presence of Pd-nanocrystallytes. Fig. 1 also shows the average crystallite size of the metallic palladium, determined by the Warren–Averbach method obtained from the licensed Win-Crysize software, which is about 3.8 nm, deduced from the half widths of the [2 0 0] reflection of metallic palladium. Also, using Topas Academic Software 4.0 nm in size was obtained for the synthesized catalysts and 25 nm for the commercial palladium (Aldrich). Fig. 2 presents an SEM image of the as-prepared catalyst. SEM analysis of the palladium powder morphology showed a rough surface with agglomerates of well-defined spherical palladium particles. Fig. 3 shows an AFM image where agglomerated particles in the range of 350 nm, whilst small particles are about 10–30 nm are observed.

3.2. Electrochemical results

The cyclic voltammetry (CV) characterization of the palladium electrode in the supporting electrolyte was performed in a nitrogen purged 0.5 mol L^{-1} H_2SO_4 solution, at 50 mV s^{-1} scan rate. In this experiment the electrode was submitted to 20 cycles

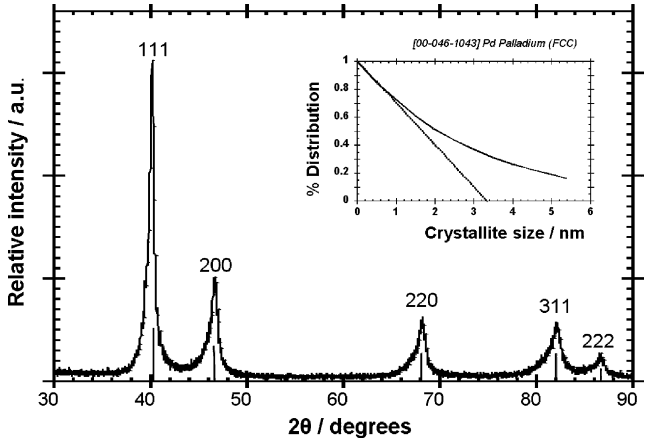

Fig. 1. XRD pattern of nanosized particles of palladium (solid lines). JCPDS card 046-1043, vertical lines. The inset shows the average crystallite size of the palladium determined by Warren–Averbach method.

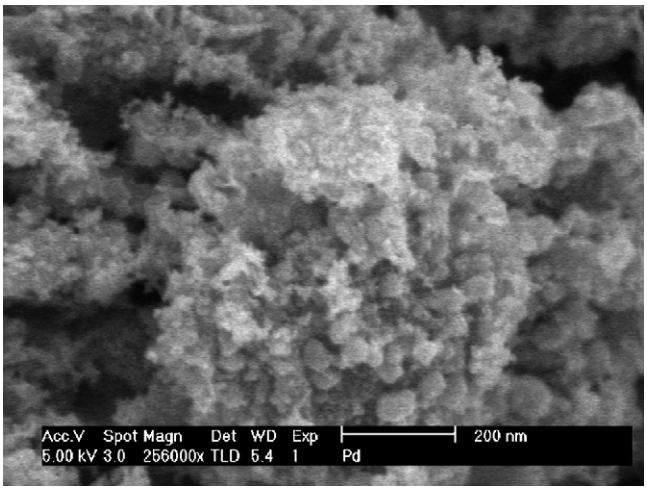

Fig. 2. SEM micrograph of as-synthesized particles of palladium, by a $NaBH_4$ reduction of $PdCl_2$ in a THF solution.

in order to obtain reproducible voltammograms. Fig. 4 presents voltammograms of different palladium samples for comparison purposes. Metallic palladium electrode presents no voltammogram peaks associated with adsorption/desorption of hydrogen characteristic in polycrystalline noble metals. However, these peaks are well-defined when the crystalline size is significantly reduced. The voltammogram of the palladium electrode with the synthesized nanoparticles showed an increase of the currents in the double layer (0.25–0.45 V) associated to the particle size. Analysis of the cathodic scan shows an increase of the oxide reduction as the catalyst particle size is being reduced. Also a higher current value in the double layer region and superior performance is maintained with nanosized palladium catalyst, demonstrated that the metal–oxygen interaction change

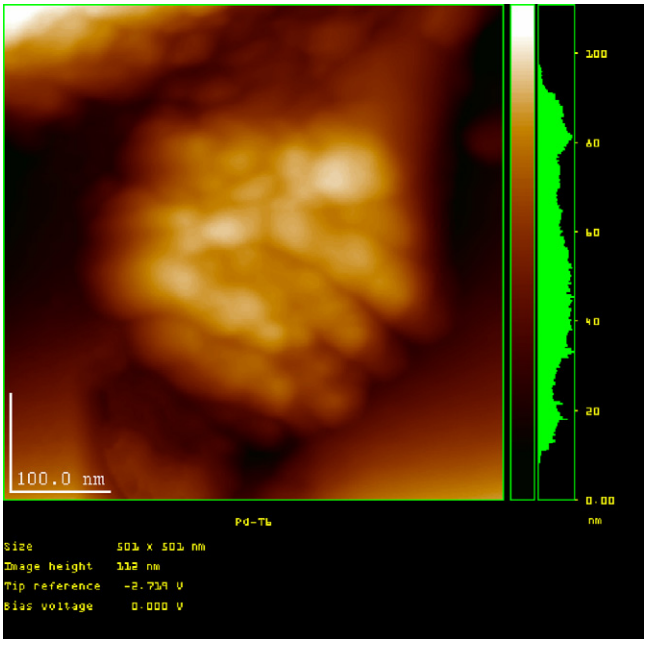

Fig. 3. AFM image of the surface morphology of the nanometric palladium catalyst.

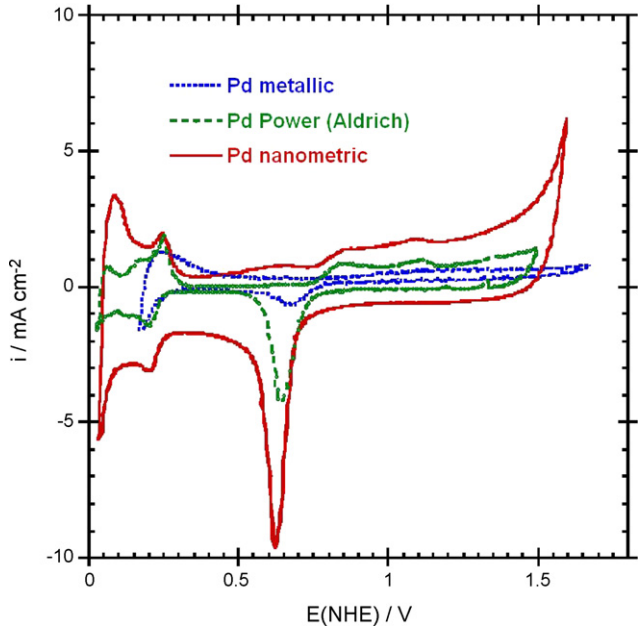

Fig. 4. Cyclic voltammograms of different palladium electrodes presentations in oxygen-free 0.5 M H_2SO_4 electrolyte. The potential was scanned at 50 mV s^{-1}.

as a function of the particle size, as pointed out in references [14,15].

Fig. 5 shows the polarization curves at different rotation rates in a different cathodic sweep of nanometric palladium incorporated into Nafion membrane electrode, in oxygen saturated 0.5 M H_2SO_4 solution at 30 °C. The main characteristic in the polarization curve is the defined charge transfer control, mixed and mass transfer region. The inset in Fig. 5 represents the inverse current density (i^{-1}) as a function of the inverse of the square root of the rotation rate ($\omega^{-1/2}$), the so-called Koutecky–Levitch plot. The linearity and parallelism of these plots indicates first-order kinetics with respect to molecular oxygen [25,26]. In a film-coated electrode surface, the overall measured density current,i, is related to the kinetic density current, i_k, the boundary layer-layer diffusion-limited density current, i_d, and film diffusion-limited current, i_f by Eq. (1). The effect of the film diffusion is significant only in the case when the electrode is covered by the Nafion film and can be neglected in the present study since the amount of Nafion (1 μL 5 wt.% Nafion in 16 μL of solution) in the prepared catalyst suspension is sufficiently small and hence not expected to be a factor in the limiting current density [26,27]. Thus, the overall measured current of the oxygen reduction can be written as being dependent on the kinetic current and the diffusion-limited current as shown in the left side of the following equation:

$$\frac{1}{i} = \frac{1}{i_k} + \frac{1}{i_d} + \frac{1}{i_f} = \frac{1}{i_k} + \frac{1}{B\omega^{1/2}} \quad (1)$$

The kinetic current density is proportional to the intrinsic activity of the catalyst. The constant B is $0.2nFCD^{2/3}v^{-1/6}$, where 0.2 is a constant used when ω is expressed in revolution per minute, C is the bulk concentration of oxygen (1.1×10^{-6} mol cm^{-3}), D is the diffusion coefficient of oxygen in the sulfuric acid solution (1.4×10^{-5} cm^2 s^{-1}) and v is the

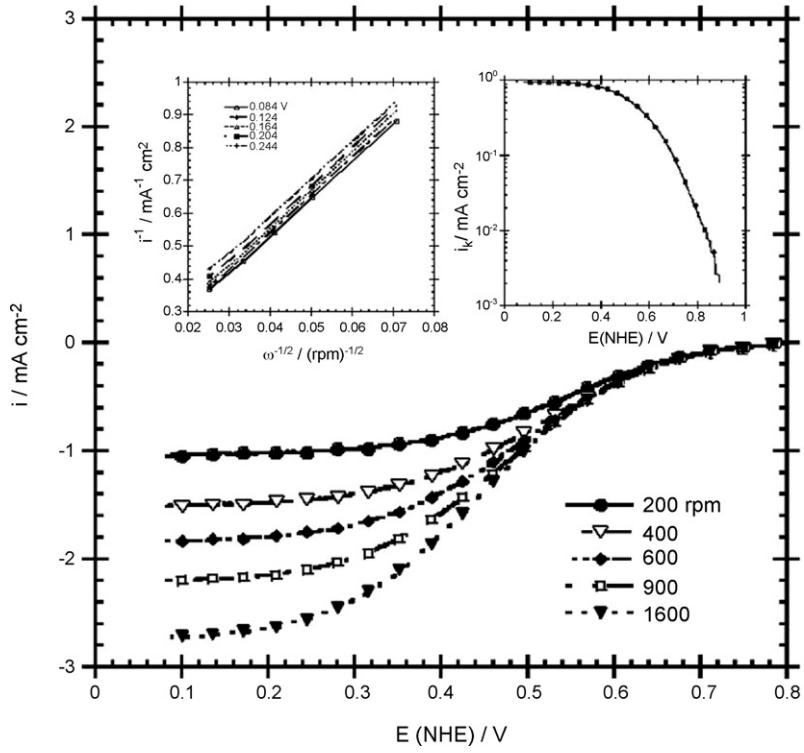

Fig. 5. Steady-state current–potential curves for ORR on Pd electrocatalyst at different rotation rates, in oxygen saturated 0.5 M H_2SO_4 electrolyte. Inset shows Koutecky–Levitch plot at various electrode potentials and mass transfer-corrected Tafel plot.

kinematic viscosity of the sulfuric acid (1.0×10^{-2} cm^{-2} s^{-1}) [28]. The slope of the straight lines inset the Fig. 5, allow us to assess the number of electrons involved in the ORR. Experimental value of ca. 11.2×10^{-2} mA rpm$^{1/2}$ obtained experimentally is in agreement with the theoretical value of 10.8×10^{-2} mA rpm$^{1/2}$ calculated for the four-electron process, indicating that the ORR on Pd nanoparticles catalyst at different potentials follows a four-electron path leading water. Tafel slope at low current density has a value of 120 mV decade^{-1} (i.e. $-2RT/F$) as expected for a first electron transfer rate determining step, and exchange current density of 6.6×10^{-6} mA cm^{-2} were determined after mass-transfer-corrected overall current, analyzing the region where the measured current density was essentially due to a mixed diffusion-kinetic control for the oxygen reduction reaction (inset Fig. 5). These results indicate that the dispersed palladium nanoparticles exhibit poor catalytic activity compared to platinum for the oxygen reduction reaction in a sulfuric acid solution. The temperature dependence on the kinetic parameters was further on examined in the range of 30–70 °C.

Fig. 6 shows the mass transfer corrected Tafel plots at several temperatures for the nanoparticles of palladium dispersed into a Nafion® membrane coating electrodes in a oxygen saturated 0.5 M H_2SO_4. Five different electrodes were prepared and tested using two different synthesized samples. The Tafel slope at each different temperature shows a linear behavior at high current density from which kinetic parameters were obtained. The increase of current densities reflect the temperature dependence of the chemical rate constant, which is approximately proportional to $e^{-\Delta H^{\circ\#}/RT}$, where $\Delta H^{\circ\#}$ is the apparent enthalpy of activation at the reversible potential. As temperature increases the onset electrode potential shifts towards high anodic values and an increase of the catalytic current density is also observed. The kinetic parameters were evaluated taking into account the reversible oxygen electrode potential at each experimental temperature [29,30]. Temperature dependence behavior of Tafel slope and transfer coefficient are shown inset Fig. 6. It is seen that there is a linear dependence of b on T with a con-

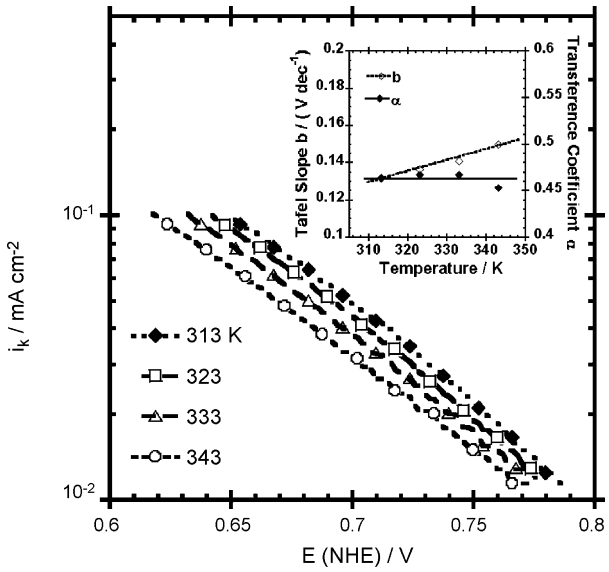

Fig. 6. Mass-transfer corrected Tafel plots for ORR at different temperatures. Inset shows the variation of Tafel slope with temperature with transfer coefficient a temperature-independent factor.

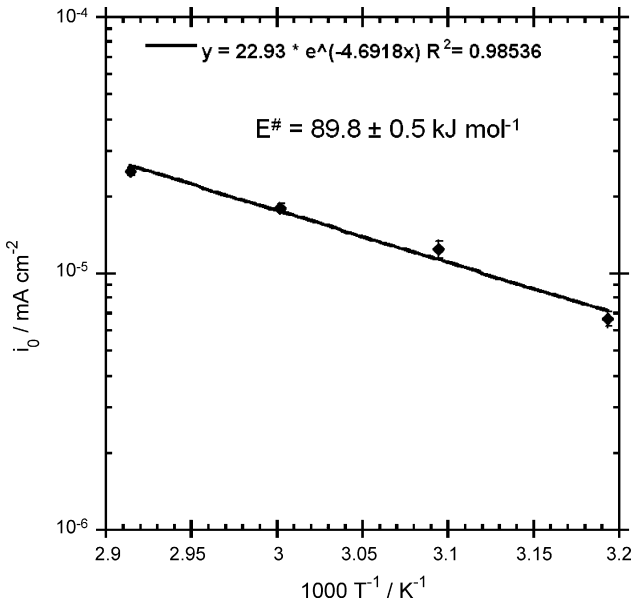

Fig. 7. Electrochemical Arrhenius plot of the exchange current density at the reversible potential for the ORR on Pd electrode.

ventional dependence of $-RT/\alpha F$ with the transfer coefficient, α, which for the oxygen reduction reaction being independent of temperature. This behavior is similar to reported and analyzed on Pt and Rh electrodes and discussed in terms of enthalpy turnover contribution to the electrocatalytic reaction [31,32]. The defined linear Tafel regions for the ORR on Pd nanoparticles were used to extrapolate the current to the theoretical equilibrium potential to obtain the exchange current densities.

The activation energy for the ORR was obtained from the exchange current density at different temperatures using the Arrhenius relationship:

$$\frac{\mathrm{d}\ \log\ i_0}{\mathrm{d}(1/T)} = -\frac{\Delta H^{\circ\#}}{2.3R} \quad (2)$$

The Arrhenius plot (log i_0 versus $1/T$) is shown in Fig. 7. An apparent enthalpy of activation $\Delta H^{\circ\#} = 89.5 \pm 0.5\,\mathrm{kJ\,mol^{-1}}$ was calculated from the average slope of their plots. This value lies in the range of activation energies reported for palladium-base electrocatalysts for the ORR in acid media [10] but it is significantly less active for the ORR than for Pt and Ru catalyst, ~20–50 kJ mol^{-1} [33,34].

4. Conclusions

The present study demonstrates that the borohydride reduction processes is an effective method for the preparation of nanometric palladium electrocatalyst. The physical characterization of the synthesized palladium showed a typical fcc hexagonal structure with agglomerated particles in an average crystallites of 4 nm in size. The effect of temperature on electrochemical parameters exhibited that the Tafel slope is directly proportional to the temperature with the transfer coefficient α a temperature-independent factor. This behavior on the electrode kinetics reveals that the enthalpy turnover of the ORR may play a significant role. Nanoparticles of palladium show a poorly catalytic activity in relation to Pt and Ru electrocatalysts in the acid media.

Acknowledgements

We gratefully acknowledge to Marco A. Leyva, Carlos Flores M and Dr. H. Yee-Madeira for technical assistance. This work was supported by the Mexican Council of Science and Technology, CONACYT, under the grand no. 46094. JJSP thanks CONACYT for bachelor fellowship.

References

[1] M. Gustavsson, H. Ekstroem, P. Hanarp, G. Lindbergh, E. Olsson, B. Kasemo, J. Power Sources 163 (2007) 671–678.
[2] J.J. Hwang, C.H. Chao, C.L. Chang, W.Y. Ho, D.Y. Wang, Int. J. Hydrogen Energy 32 (2007) 405–414.
[3] K.S. Nagabhushana, C. Wiedenthaler, S. Hocevar, D. Strmcnik, M. Gaberscek, A.L. Antozzi, G.N. Martelli, J. New Mater. Electrochem. Syst. 9 (2006) 73–81.
[4] M.R. Tarasevich, K.A. Radyushkina, G.V. Zhutaeva, Rus. J. Electrochem. 40 (2004) 1369–1383.
[5] D. Villers, X.J. -Bédard, J.-P. Dodelet, J. Electrochem. Soc. 151 (2004) A1507–A1515.
[6] S. Doi, A. Ishihara, S. Mitsushima, N. Kamiya, K. Ota, J. Electrochem. Soc. 154 (2007) B362–B369.
[7] J. Maruyama, I. Abe, J. Electrochem. Soc. 154 (2007) B297–B304.
[8] J. Pettersson, B. Ramsey, D. Harrison, J. Power Sources 157 (2006) 28–34.
[9] L. Zhang, K. Lee, J. Zhang, Electrochim. Acta 52 (2007) 3088–3094.
[10] W.E. Mustain, K. Kepler, J. Prakash, Electrochim. Acta 52 (2007) 2102–2108.
[11] M.R. Tarasevich, A.E. Chalykh, V.A. Bogdanovskaya, L.N. Kuznetsova, N.A. Kapustina, B.N. Efremov, M.R. Ehrenburg, L.A. Reznikova, Electrochim. Acta 51 (2006) 4455–4462.
[12] L.D. Burbe, J.K. Casey, J. Electrochem. Soc. 140 (1993) 1284–1291.
[13] V. Raghuveer, P.J. Ferreira, A. Manthiram, Electrochem. Commun. 8 (2006) 807–814.
[14] O. Savadogo, K. Lee, K. Oishi, S. Mitsushima, N. Kamiya, K.-I. Ota, Electrochem. Commun. 6 (2004) 105–109.
[15] J.L. Fernandez, J.M. White, Y. Sun, W. Tang, G. Henkelman, A.J. Bard, Langmuir 22 (2006) 10426–10431.
[16] M.H. Shao, T. Huang, P. Liu, J. Zhang, K. Sasaki, M.B. Vukmirovic, R.R. Adzic, Langmuir 22 (2006) 10409–10415.
[17] M.-H. Shao, K. Sasaki, R.R. Adzic, J. Am. Chem. Soc. 128 (2006) 3526–3527.
[18] M.S. Chen, D.W. Goodman, Science 306 (2004) 252–255.
[19] R. Meyer, C. Lemire, Sh.K. Shaikhutdinov, H.-J. Freund, Gold Bull. 37 (2004) 72–124.
[20] R. Suryanarayanan, C.A. Frey, S.M.L. Sastry, B.E. Waller, S.E. Bates, W.E. Buhro, J. Mater. Res. 11 (1996) 439–448.
[21] J. Prabhuram, T.S. Zhao, Z.K. Tang, R. Chen, Z.X. Liang, J. Phys. Chem. B. 110 (2006) 5245–5252.
[22] B. Veisz, L. Tóth, D. Teschner, Z. Paál, N. Gyorffy, U. Wild, R. Schlogl, J. Mol. Catal. A: Chem. 238 (2005) 56–62.
[23] R.G. Gonzalez-Huerta, R. González-Cruz, S. Citalán-Cigarroa, C. Montero-Ocampo, J. Chavez-Carvayar, O. Solorza-Feria, J. New Mater. Electrochem. Syst. 8 (2005) 15–23.
[24] R.G. González-Huerta, A. Chávez-Carvayar, O. Solorza-Feria, J. Power Sources 153 (2006) 11–17.
[25] A.J. Bard, L. Faulkner, Electrochemical Methods: Fundamentals and Applications, Wiley, New York, 2001, pp. 340–344.
[26] K. Suárez-Alcántara, A. Rodríguez-Castellanos, R. Dante, O. Solorza-Feria, J. Power Sources 157 (2006) 114–120.

[27] V.S. Murthi, R.C. Urian, S. Mukerjee, J. Phys. Chem. B 108 (2004) 11011–11023.
[28] C. Couteanceau, P. Crouigneau, J.-M. Léger, C. Lamy, J. Electroanal. Chem. 379 (1994) 389–397.
[29] A. Parthasarathy, S. Srinivasan, A.J. Appleby, C.R. Martin, J. Electrochem. Soc. 139 (1992) 2530–2537.
[30] N. Alonso-Vante, H. Tributsch, O. Solorza-Feria, Electrochim. Acta 40 (1995) 567–576.
[31] A. Damjanovic, in: O.J. Murphy, S. Srinivasan, B.E. Conway (Eds.), Electrochemistry in Transition from the 20th to the 21st Century, Plenum Press, New York, 1992, pp. 107–126.
[32] D.B. Sepa, V. Vojnovic, M. Stojanovic, A. Damjanovic, J. Electrochem. Soc. 134 (1987) 845–848.
[33] K. Kinoshita, Electrochemical Oxygen Technology, John Wiley & Sons, New York, 1998, pp. 197–242.
[34] O. Solorza-Feria, S. Durón, Int. J. Hydrogen Energy 27 (2002) 451–455.